GEOPHYSICAL RESEARCH LETTERS, VOL. 39, L18405, doi:10.1029/2012GL052988, 2012

Evaluating global trends (1988–2010) in harmonized multi-satellite surface soil moisture

Wouter Dorigo,[1] Richard de Jeu,[2] Daniel Chung,[1] Robert Parinussa,[2] Yi Liu,[3,4] Wolfgang Wagner,[1] and Diego Fernández-Prieto[5]

Received 3 July 2012; revised 13 August 2012; accepted 14 August 2012; published 26 September 2012.

[1] Global trends in a new multi-satellite surface soil moisture dataset were analyzed for the period 1988–2010. 27% of the area covered by the dataset showed significant trends (p = 0.05). Of these, 73% were negative and 27% positive. Subtle drying trends were found in the Southern US, central South America, central Eurasia, northern Africa and the Middle East, Mongolia and northeast China, northern Siberia, and Western Australia. The strongest wetting trends were found in southern Africa and the subarctic region. Intra-annual analysis revealed that most trends are not uniform among seasons. The most prominent trend patterns in remotely sensed surface soil moisture were also found in GLDAS-Noah and ERA Interim modeled surface soil moisture and GPCP precipitation, lending confidence to the obtained results. The relationship with trends in GIMMS-NDVI appeared more complex. In areas of mutual disagreement more research is needed to identify potential deficiencies in models and/or remotely sensed products. **Citation:** Dorigo, W., R. de Jeu, D. Chung, R. Parinussa, Y. Liu, W. Wagner, and D. Fernández-Prieto (2012), Evaluating global trends (1988–2010) in harmonized multi-satellite surface soil moisture, *Geophys. Res. Lett.*, *39*, L18405, doi:10.1029/2012GL052988.

1. Introduction

[2] Soil moisture is one of the main drivers of the exchange of water, energy, and carbon between the land surface and atmosphere [*Jung et al.*, 2010]. Encapsulating precipitation, evaporation, infiltration, and runoff it is a suited state variable for studying climate variability and the severity and duration of drought events [*Dai*, 2011; *De Jeu et al.*, 2012]. For this reason, observing soil moisture has been set high on the agenda of the Global Climate Observing System (GCOS) by endorsing it as an Essential Climate Variable [*GCOS*, 2010].

[3] Traditionally, trends and dynamics in soil moisture have been studied from sparse ground-based measurements [*Robock et al.*, 2005]. As in-situ measurements commonly lack global coverage and representativeness, recent studies have mostly relied on model estimates [*Sheffield and Wood*, 2008; *Zhu and Lettenmaier*, 2007]. Nevertheless, for many regions of the world land-atmosphere feedback mechanisms are not yet well understood [*Taylor et al.*, 2012] and, as a result, soil moisture model estimates in these regions may be prone to large uncertainties [*Ferguson and Wood*, 2011].

[4] Satellite-based surface soil moisture datasets from active and passive microwave sensors [e.g., *Bartalis et al.*, 2007; *Njoku et al.*, 2003; *Owe et al.*, 2008] open up the possibility to study the global behavior of soil moisture from 1979 onwards from observational data alone. Despite sensing only the upper few centimeters of the soil, the datasets usually show a strong relationship with deeper layers [*Albergel et al.*, 2008]. However, none of the individual microwave products covers the full time period needed for a climate record or the global spatial domain, while differences in system and mission design and the use of different retrieval algorithms have led to varying quality over space and time [*Dorigo et al.*, 2010; *Parinussa et al.*, 2011]. A first attempt to merge soil moisture products from different active and passive microwave satellite sensors into a single dataset covering the period 1979–2010 was made by *Liu et al.* [2011b, 2012]. Based on this dataset our study for the first time globally assesses structural, multi-decadal changes in surface soil moisture from observational data alone. We compared the observed trends with trends over the same period in two model-based surface soil moisture datasets, a precipitation dataset, and a vegetation dataset in order to identify consistencies and potential shortcomings in the various datasets.

2. Data and Methods

2.1. Homogenized Remotely Sensed Soil Moisture

[5] Trend analysis is based on the merged microwave-based surface soil moisture dataset (SM-MW) presented by *Liu et al.* [2011b, 2012]. It combines radiometer-based products from SMMR (November 1978–August 1987), SSM/I (July 1987–2007), TMI (1998–2008), and AMSR-E (July 2002–2010) with scatterometer-based products from ERS-1/2 (July 1991–May 2006) and ASCAT (2007–2010). The datasets are merged based on their relative sensitivity to vegetation density. SM-MW is expressed in a reference climatology provided by the GLDAS-Noah surface soil moisture product [*Rodell et al.*, 2004]. *Liu et al.* [2012] showed that even though this procedure affects the absolute soil moisture values, dynamics and trends in the remote

[1]Institute of Photogrammetry and Remote Sensing, Vienna University of Technology, Vienna, Austria.
[2]Department of Earth Sciences, Faculty of Earth and Life Sciences, VU University Amsterdam, Amsterdam, Netherlands.
[3]Water Research Centre, School of Civil and Environmental Engineering, University of New South Wales, Sydney, New South Wales, Australia.
[4]Black Mountain Laboratories, CSIRO Land and Water, Canberra, ACT, Australia.
[5]ESRIN, European Space Agency, Frascati, Italy.

Corresponding author: W. Dorigo, Institute of Photogrammetry and Remote Sensing, Vienna University of Technology, Gusshausstrasse 27-29, A-1040 Vienna, Austria. (wd@ipf.tuwien.ac.at)

0094-8276/12/2012GL052988

sensing data are preserved while potential trends in GLDAS-Noah soil moisture are not imposed on the merged product. SM-MW has a spatial resolution of 0.25°, a daily time stamp, and represents the upper few (~2) cm of the soil. SM-MW is known to fail over dense vegetation, and uncertainty increases for earlier periods [*Dorigo et al.*, 2010; *Liu et al.*, 2012].

[6] The scaling and merging approach relies on the common observation periods between sensors. SMMR (1978–1987) has only a very short overlap with the successive SSM/I sensor, making a trend-preserving match with later datasets impossible [*Liu et al.*, 2012]. Therefore, the SMMR period was excluded from this study and trend analyses were based on the period 1988–2010. Daily observations were filtered for soil frost and then averaged into seasonal values: December–February (DJF), March–May (MAM), June–August (JJA), and September–November (SON).

2.2. Modeled Soil Moisture

[7] Soil moisture estimates as provided by the ERA Interim reanalysis dataset [*Dee et al.*, 2011] and the Global Land Data Assimilation System (GLDAS) Noah model [*Rodell et al.*, 2004] were used to cross-validate the trends observed in SM-MW. ERA Interim provides several atmospheric and surface fields for the period 1979–present by assimilating various types of observations including satellite and ground-based measurements. Fields are generated every six hours at a spatial resolution of ~80 km. Land surface processes are described by four different layers of a globally uniform soil. For this study we used soil moisture simulations of the upper layer (0–0.07 m).

[8] GLDAS-Noah provides atmospheric and land surface variables at a three-hour time interval. The model is forced by a combination of atmospheric analysis, satellite-based precipitation, and observation-based radiation fields. The soil profile is represented by four vertical layers of which the upper one (0–0.10 m) is used in this study. GLDAS-Noah adopts spatially variable soil properties derived from a global soil database. We used the reduced resolution version (1.0°) which covers the entire 1988–2010 period considered in this study. After filtering for negative soil temperatures and snow cover, the soil moisture estimates of both products were averaged into seasonal means, similar as for SM-MW.

2.3. Remotely Sensed Precipitation and Vegetation

[9] Preciptation is one of the main drivers of variations in surface soil moisture [*Lakshmi*, 2004]. Therefore, we compared the trends observed in SM-MW with those computed from the Global Precipitation Climatology Project (GPCP) Version 2.2 [*Adler et al.*, 2003]. GPCP merges data from over 6,000 rain gauge stations with various types of satellite observations into a monthly 2.5° resolution rainfall product from 1979–present. The monthly estimates were binned into three-monthly cumulative precipitation amounts.

[10] The Normalized Difference Vegetation Index (NDVI) can be used as a proxy for vegetation development [*Dorigo et al.*, 2007]. As vegetation development is sensitive primarily to root-zone soil moisture, long-term changes in the latter should be reflected by structural changes in NDVI. We used the NDVI as provided by the long-term AVHRR-based Global Inventory Monitoring and Modeling Studies (GIMMS) 3g version [*Tucker et al.*, 2005].

2.4. Trend Analysis

[11] Trends in all datasets were calculated using the non-parametric Mann-Kendall test which has been widely used in detecting monotonic trends in environmental time series [e.g., *Liu et al.*, 2011a; *Sheffield and Wood*, 2008]. The test does not require any assumptions about the distribution of the data or the form of the trend [*Helsel and Hirsch*, 1992]. Prerequisite for the test is that individual data values are uncorrelated. This condition holds for the use of seasonal means as autocorrelation time lengths of remotely sensed surface moisture have been found to remain well below three months [*Rebel et al.*, 2012]. We used the implementation proposed by *Sen* [1968] which is more robust to outliers. The test provides a statistic which is used to calculate its significance (p-value) with respect to a Gaussian distribution around zero mean (no change). To test for consistency between trends in SM-MW and those observed in the evaluation datasets we adopted the test that this commonly used to test for homogeneity within the seasonal Mann-Kendall test [*Gilbert*, 1987, chap. 17].

3. Results and Discussion

3.1. Trends in Remotely Sensed Surface Soil Moisture

[12] Figure 1 shows the global trends ($m^3m^{-3}y^{-1}$) calculated from SM-MW. Only significant trends ($p = 0.05$) are shown, which total 27% of the total number of pixels with valid soil moisture time series. The global picture is dominated by decreasing surface soil moisture contents over time. While for the entire dataset 59% of the trends are negative (drying), this number is 73% if only significant trends are considered. Most prominent drying trends occur over the southern United States, central South America, northern Africa and the Middle East, central Eurasia, northern Siberia, northeast China and Mongolia, and northwestern Australia. Many of the strong drying trends occur in regions which already have relatively low average soil moisture values (Figure 1b). The most prominent wetting trend is observed for central southern Africa, while spatially less extensive positive trends are observed for Northern Canada, the area around Lake Winnipeg, the Baltic States and Belarus, northeast Siberia, eastern China, and along Australia's east coast. Figure S1 in the auxiliary material provides some examples of time series for areas with significant trends.[1]

[13] Whether the observed trends are systematic or caused by protracted extreme events is still focus of research. For example, *Dole et al.* [2011] concluded that the 2010 Russian heat wave, which is reflected in our soil moisture trends, was caused by natural atmospheric variability. Likewise, the Australian "Big Dry" was mostly driven by various ocean oscillation systems [*Verdon-Kidd and Kiem*, 2009]. At the same time, many of the structural trends observed in our study confirm the work of *Sheffield and Wood* [2008], especially in high northern latitudes. There is also a remarkable resemblance with the negative trends in evapotranspiration observed by *Jung et al.* [2010] over moisture-limited regions.

[1]Auxiliary materials are available in the HTML. doi:10.1029/2012GL052988.

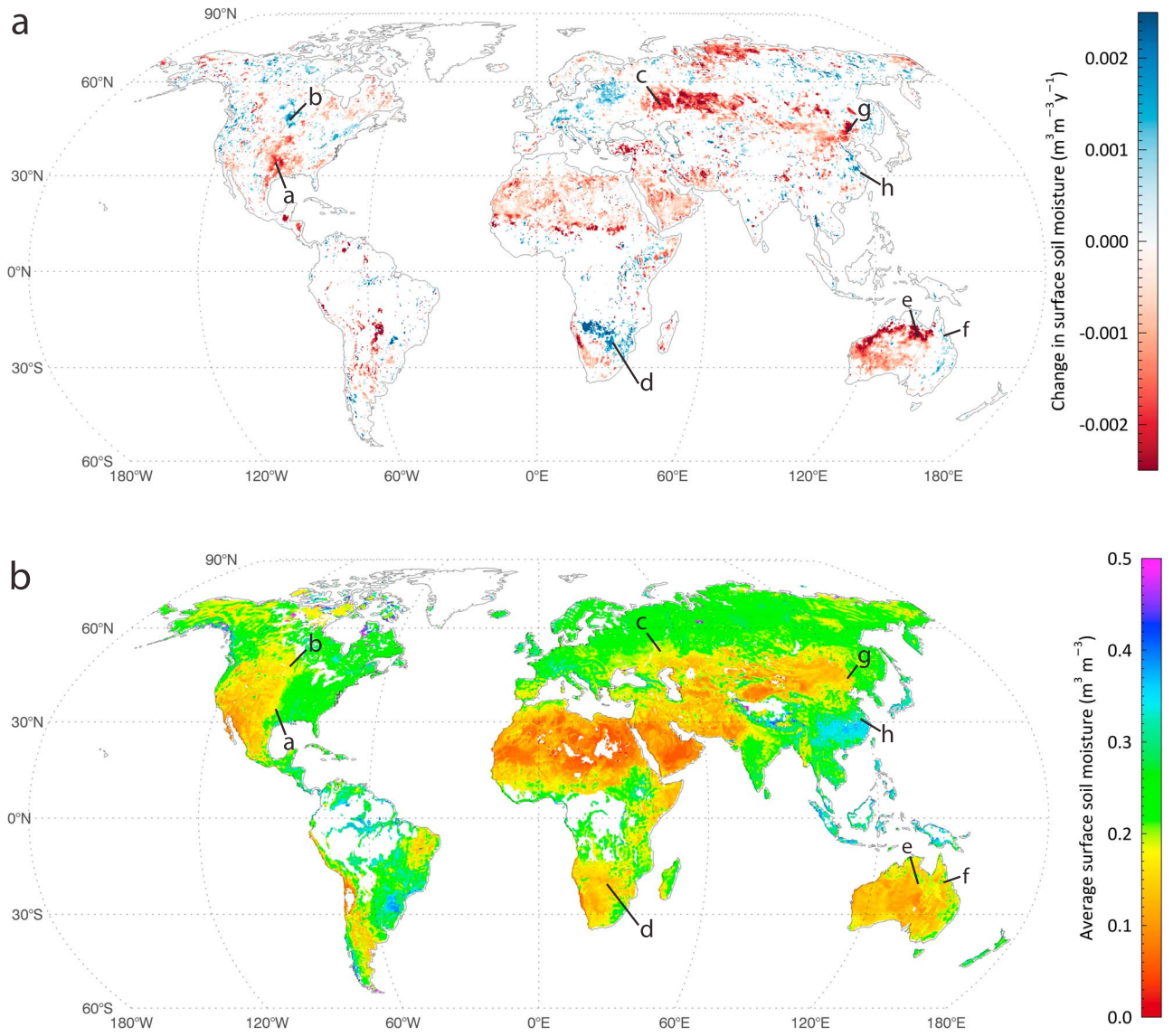

Figure 1. (a) Changes in SM-MW ($m^3\ m^{-3}\ y^{-1}$) over the period 1988–2010 based on the Mann-Kendall trend test. Only trends significant at p = 0.05 are shown. (b) Average SM-MW over the same period. The numbers show the locations of the time series plots in the auxiliary material.

3.2. Seasonal Trends

[14] For regions of the world with pronounced seasonal cycles, such as monsoon regions and continental interiors, trends are likely to vary by season. Therefore, trend values were computed for each season separately. Figure 2 shows that for several regions trends are consistent (though somewhat varying in extent) for all four seasons, e.g., large parts of the southern United States, parts of northern Africa and the Middle East, northeastern China and Mongolia, and northwestern Australia. Apart from the winter season, when due to frozen soils and snow cover soil moisture cannot be remotely mapped, the strong negative trend in central Eurasia is persistent throughout the year. This is consistent with the temperature records analyzed by *Dole et al.* [2011].

[15] Several trends observed in Figure 1 are not consistent for all seasons, e.g., the overall drying trend observed in Southern America is mainly driven by an obvious drying trend at the end of the dry season (MAM). Many regions also exhibit strong contrasting seasonal trends that counterbalance each other at a yearly level. The most striking example is observed for South China where a strong negative trend observed for the local dry season (DJF) is compensated by a strong positive trend for the onset of the wet season (MAM). This may be an indication that the contrast between dry and wet periods exacerbates in some regions. The opposite effect, i.e., a dampening the contrast between the seasons, is observed in southern Africa where the strong wetting trend observed in Figure 1 seems to be largely driven by the positive trend over the regional dry season (JJA). A similar phenomenon, but with a seasonal shift related to the annual cycle of the Intertropical Convergence Zone (ITCZ), seems to occur in the northern African Sahel region. Recent strong anomalous seasonal behavior of soil moisture in both regions was already observed by [*De Jeu et al.*, 2011, 2012].

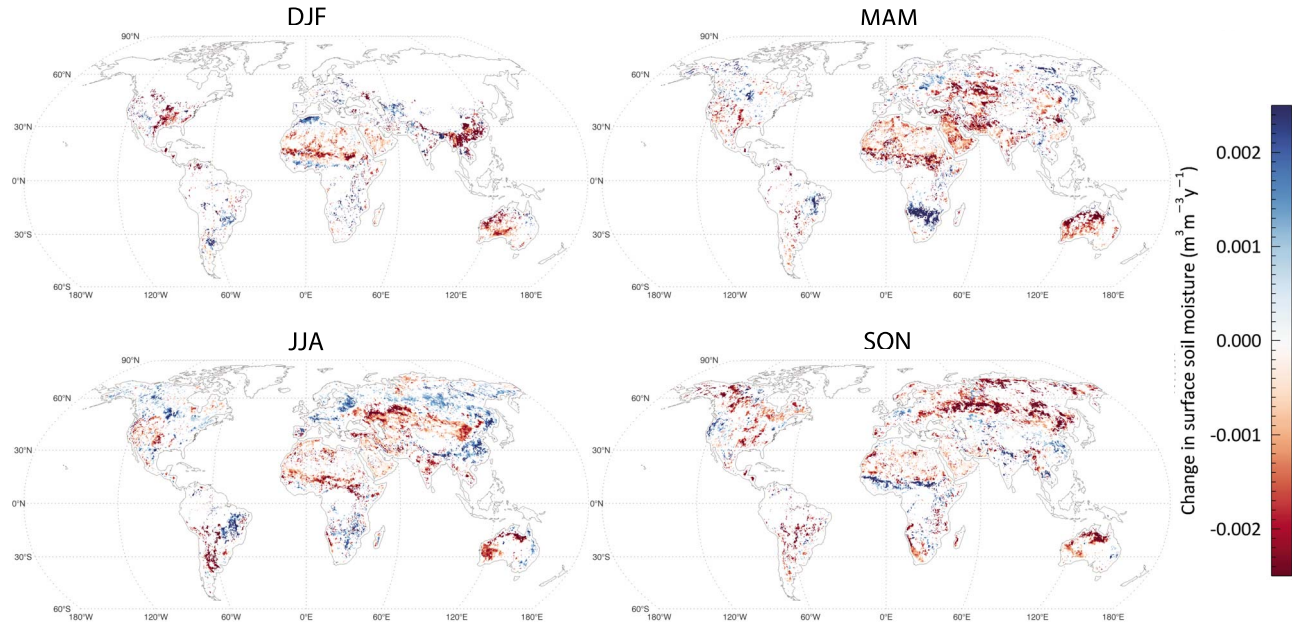

Figure 2. Trend in SM-MW ($m^3\ m^{-3}\ y^{-1}$) over the period 1988–2010 split up per season. Only trends that are significant at p = 0.05 are shown.

3.3. Consistency With Global Trends in Model Surface Soil Moisture, Precipitation, and NDVI

[16] The patterns in SM-MW trends are generally confirmed by the modeled surface soil moisture datasets (Figure 3, left). However, percentages of unfiltered negative trends for the pixels covered by SM-MW are significantly higher for the modeled datasets, especially for GLDAS-Noah (Table 1). Approximately 56% of the SM-MW trends agree in sign with either of the evaluation datasets, while ~18% of the globally measured SM-MW trends agree in sign with the modeled datasets and are significant at p = 0.05. This percentage is slightly lower if also the significance of the consistency in trends between SM-MW and modeled soil moisture after *Gilbert* [1987] is considered. After filtering for this consistency most prominent patterns identified in Figure 1 persist (Figure 3, right). Consistencies in negative trends with both ERA-Interim and GLDAS-Noah are found for the southern US, central and southern South America, the Middle East, central Eurasia, northern Siberia, northeastern China and Mongolia, and northwestern Australia. The most prominent wetting trend in southern Africa is also seen in the modeled datasets, although with a reduced spatial extent. Also the positive trends in northern Canada and around Lake Winnipeg are represented by the model datasets. Some of the clear trends in the remote sensing data, e.g., the wetting trends in the Baltic countries and along Australia's east coast, and the strong negative trend in western Namibia, are not reproduced by the modeled datasets. In other cases the trend in SM-MW is reproduced by one of the model datasets but not by the other, e.g., in large part of the Sahara and eastern Africa. This clearly shows that models still disagree over many parts of the globe and that additional efforts are needed to verify the quality of model output. Even though land surface model estimates datasets generally respond well to short-term variations [*Albergel et al.*, 2012a; *Reichle et al.*, 2011], little is known about their capability of reproducing interannual variations and trends [*Simmons et al.*, 2010]. Observational datasets like the one presented in this study can be used to test and revise the processes and parameterizations used to calculate the water balance at the surface, which are known sometime to be inadequate for ERA Interim [*Albergel et al.*, 2012b].

[17] At first sight, trend patterns of precipitation look different from those observed for SM-MW and modeled surface soil moisture. In fact, the majority of precipitation trends over locations for which SM-MW is available are positive. Nevertheless, the major negative (Southern US, southern South America, the Middle East, central Eurasia, northern Siberia, Mongolia and northeastern China) and positive (northern Canada, area around Lake Winnipeg, southern Africa) soil moisture trends are also picked up by the precipitation dataset. This confirms that major surface soil moisture variations are mainly precipitation driven, especially in moisture-limited areas [*Jung et al.*, 2010]. The SM-MW trends in northwestern Australia and North Africa could only be partly confirmed by GPCP. Interestingly, some of the significant wetting trends in SM-MW that were not captured by the two model datasets, i.e., in the Baltic states and Belarus, and in northeast Siberia, do appear in the GPCP dataset.

[18] The most evident agreement between NDVI and SM-MW is found for southern South America, central Eurasia, and Mongolia, and northeastern China. Also the general wetting patterns around Lake Winnipeg, in the Baltic States, and in Western China are reflected by the NDVI data. However, the ubiquitous drying trends in the Southern US and Australia, and the pronounced positive trend in southern Africa are not so obvious in the NDVI data. The exact processes behind the differences are still focus of study, although it is likely that land cover plays a crucial role in this

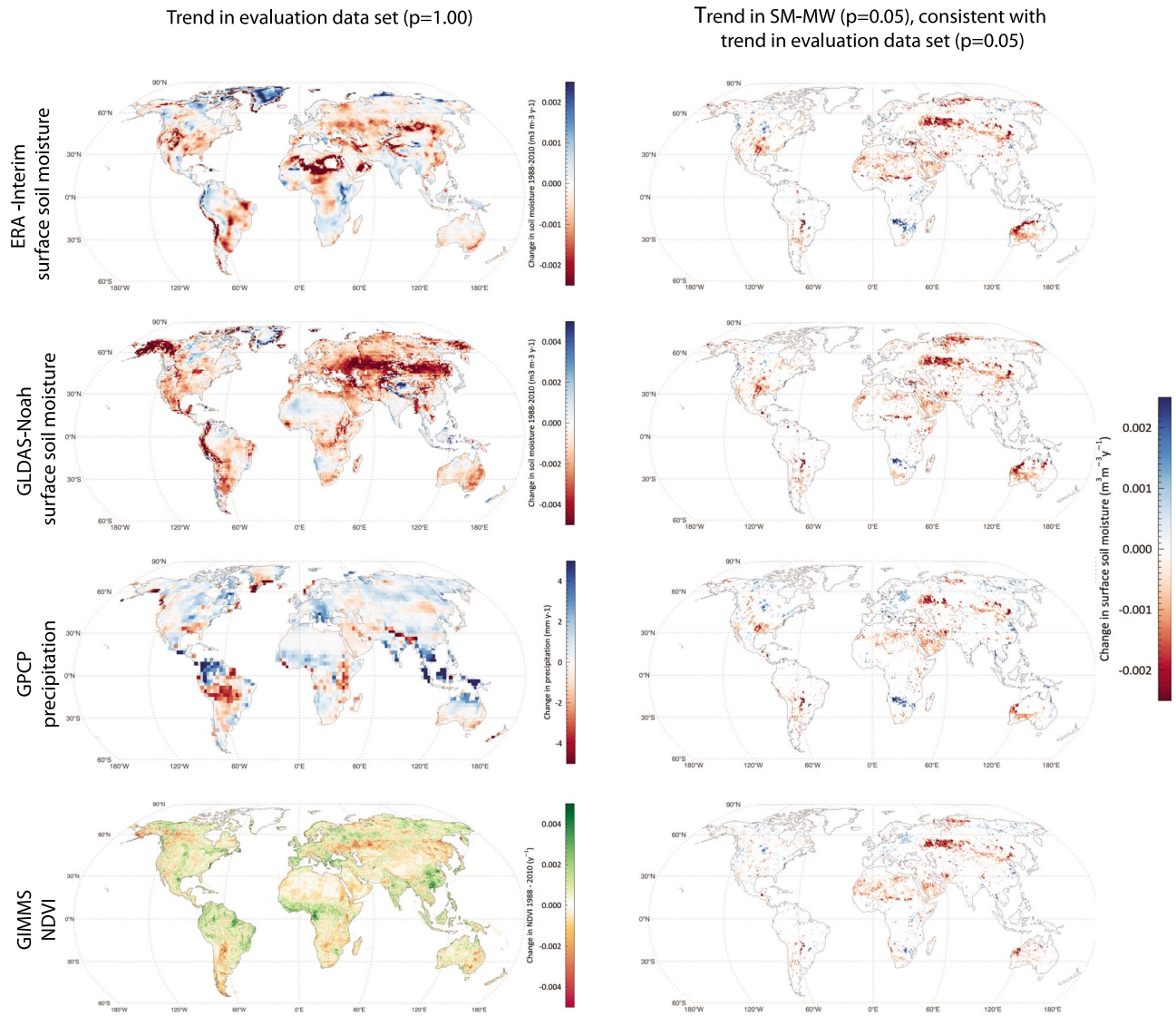

Figure 3. (left) Trends in ERA-Interim surface soil moisture, GLDAS-Noah surface soil moisture, GPCP precipitation, and GIMMS NDVI for the period 1988–2010. (right) Trends in SM-MW (p = 0.05) that agree significantly (p = 0.05) with trends in the evaluation datasets.

respect, with crops reacting more directly to changes in available water than bushes and trees [*Liu et al.*, 2011a].

4. Conclusion

[19] For the first time, global trends (1988–2010) in a new merged satellite-based surface soil moisture product (SM-MW) were analyzed and compared with trends in two model-based surface soil moisture products, a precipitation, and an NDVI dataset. Most of the major trends in SM-MW were also visible in the other datasets, although spatial extents generally deviated. In all soil moisture datasets a strong tendency towards drying was observed while this

Table 1. Trends in Evaluation Datasets and Agreement Between Trends in Evaluation Datasets and Trends in SM-MW (in % of Total Number of Grid Points Covered by SM-MW)

	ERA-Interim Surface Soil Moisture	GLDAS-Noah Surface Soil Moisture	GPCP Precipitation	GIMMS NDVI
Percentage of positive/negative trends	31/69	20/80	59/41	45/55
Sign of trends coincides	57	57	53	52
Sign coincides, trend SM-MW is significant (p = 0.05)	18	18	15	15
Sign coincides, trend SM-MW is significant (p = 0.05), trends in both datasets agree significantly (p = 0.05)	15	16	9	12

could not be confirmed by the precipitation dataset. This shows that even though precipitation is the main driver of variations in soil moisture, its impact is controlled by evaporation, soil type, irradiation, vegetation, and topography. Most of the dominant trend patterns were also confirmed by trends in NDVI, which was used as a proxy of root-zone soil moisture. This observation suggests that surface soil moisture is suited to study structural moisture changes in the entire soil column. Nevertheless, the relationship between SM-MW and NDVI is not as straightforward as for the other datasets since vegetation type, and changes herein, play a crucial role.

[20] Many of the most evident SM-MW trends, such as in central Eurasia, southern South America, and northern Siberia, were confirmed by all evaluation datasets, which evidences the reliability of the results in these areas. The most remarkable contradicting result is obtained in northern and southeastern Australia. While SM-MW shows an obvious drying (north) and wetting (southeast) trend, all other datasets show evidence of reversed conditions. Further research is needed to study the causes of this discrepancy.

[21] Despite the promising results, the reader should be aware of the limitations and uncertainties of the merged dataset. SM-MW relies on sensors with differences in temporal resolution and coverage, spatial resolution, observation principle, sensor calibration, center frequencies, band width, and radiometric accuracy. In addition, the performance of the retrieval algorithms is sensitive to topography, surface water, and vegetation while retrievals entirely fail for dense vegetation. Therefore, our future research will focus on improving our understanding of product uncertainties and their potential effect on the observed trends. Moreover, additional evaluation datasets will help us to unveil some of the inconsistencies between the datasets in this study and to identify the drivers of the observed trends.

[22] **Acknowledgments.** GPCP precipitation data were provided by the NOAA/OAR/ESRL PSD, Boulder, Colorado, USA. This study was performed in the framework of the STSE Water Cycle Multimission Observation Strategy (WACMOS) project funded by the European Space Agency (contract 22086/08/1-EC) and ESA's Climate Change Initiative for Soil Moisture (contract 4000104814/11/I-NB). We thank Jorge Pinzon and Jim Tucker (NASA, Goddard Space Flight Center) for providing access to the NDVI GIMMS3g dataset.

[23] The editor thanks Clement Albergel and an anonymous reviewer for their assistance evaluating this manuscript.

References

Adler, R. F., et al. (2003), The version-2 global precipitation climatology project (GPCP) monthly precipitation analysis (1979–present), *J. Hydrometeorol.*, *4*(6), 1147–1167, doi:10.1175/1525-7541(2003)004<1147:TVGPCP>2.0.CO;2.

Albergel, C., C. Rüdiger, T. Pellarin, J. C. Calvet, N. Fritz, F. Froissard, D. Suquia, A. Petitpa, B. Piguet, and E. Martin (2008), From near-surface to root-zone soil moisture using an exponential filter: An assessment of the method based on in-situ observations and model simulations, *Hydrol. Earth Syst. Sci.*, *12*(6), 1323–1337, doi:10.5194/hess-12-1323-2008.

Albergel, C., P. De Rosnay, G. Balsamo, L. Isaksen, and J. Munoz-Sabater (2012a), Soil moisture analyses at ECMWF: Evaluation using global ground-based in situ observations, *J. Hydrometeorol.*, doi:10.1175/JHM-D-11-0107.1, in press.

Albergel, C., P. de Rosnay, C. Gruhier, J. Muñoz-Sabater, S. Hasenauer, L. Isaksen, Y. Kerr, and W. Wagner (2012b), Evaluation of remotely sensed and modelled soil moisture products using global ground-based in situ observations, *Remote Sens. Environ.*, *118*, 215–226, doi:10.1016/j.rse.2011.11.017.

Bartalis, Z., W. Wagner, V. Naeimi, S. Hasenauer, K. Scipal, H. Bonekamp, J. Figa, and C. Anderson (2007), Initial soil moisture retrievals from the METOP-A Advanced Scatterometer (ASCAT), *Geophys. Res. Lett.*, *34*, L20401, doi:10.1029/2007GL031088.

Dai, A. (2011), Drought under global warming: A review, *Wiley Interdiscip. Rev. Clim. Change*, *2*(1), 45–65, doi:10.1002/wcc.81.

De Jeu, R., W. Dorigo, W. Wagner, and Y. Liu (2011), Global climate soil moisture, *Bull. Am. Meteorol. Soc.*, *92*(6), S52–S53.

De Jeu, R., W. Dorigo, R. M. Parinussa, W. Wagner, and D. Chung (2012), Global climate soil moisture, *Bull. Am. Meteorol. Soc.*, *93*(7), S30–S34.

Dee, D. P., et al. (2011), The ERA-Interim reanalysis: Configuration and performance of the data assimilation system, *Q. J. R. Meteorol. Soc.*, *137*(656), 553–597, doi:10.1002/qj.828.

Dole, R., M. Hoerling, J. Perlwitz, J. Eischeid, P. Pegion, T. Zhang, X. W. Quan, T. Xu, and D. Murray (2011), Was there a basis for anticipating the 2010 Russian heat wave?, *Geophys. Res. Lett.*, *38*, L06702, doi:10.1029/2010GL046582.

Dorigo, W. A., R. Zurita-Milla, A. J. W. de Wit, J. Brazile, R. Singh, and M. E. Schaepman (2007), A review on reflective remote sensing and data assimilation techniques for enhanced agroecosystem modeling, *Int. J. Appl. Earth Obs.*, *9*(2), 165–193, doi:10.1016/j.jag.2006.05.003.

Dorigo, W. A., K. Scipal, R. M. Parinussa, Y. Y. Liu, W. Wagner, R. A. M. de Jeu, and V. Naeimi (2010), Error characterisation of global active and passive microwave soil moisture data sets, *Hydrol. Earth Syst. Sci.*, *14*, 2605–2616, doi:10.5194/hess-14-2605-2010.

Ferguson, C. R., and E. F. Wood (2011), Observed land-atmosphere coupling from satellite remote sensing and reanalysis, *J. Hydrometeorol.*, *12*(6), 1221–1254, doi:10.1175/2011JHM1380.1.

GCOS (2010), Implementation plan for the Global Observing System for climate in support of the UNFCCC—2010 update, report, World Meteorol. Organ., Geneva Switzerland.

Gilbert, R. O. (1987), *Statistical Methods for Environmental Pollution Monitoring*, 1st ed., 320 pp., Wiley, New York.

Helsel, D. R., and R. M. Hirsch (1992), Statistical methods in water resources, *U.S. Geol Surv. Tech. Water Resour. Invest.*, *Book 4*, *Chap. A3*, 522 pp.

Jung, M., et al. (2010), Recent decline in the global land evapotranspiration trend due to limited moisture supply, *Nature*, *467*(7318), 951–954, doi:10.1038/nature09396.

Lakshmi, V. (2004), The role of satellite remote sensing in the prediction of ungauged basins, *Hydrol. Processes*, *18*(5), 1029–1034, doi:10.1002/hyp.5520.

Liu, Y. Y., R. A. M. de Jeu, M. F. McCabe, J. P. Evans, and A. I. J. M. van Dijk (2011a), Global long-term passive microwave satellite-based retrievals of vegetation optical depth, *Geophys. Res. Lett.*, *38*, L18402, doi:10.1029/2011GL048684.

Liu, Y. Y., R. M. Parinussa, W. A. Dorigo, R. A. M. De Jeu, W. Wagner, A. I. J. M. Van Dijk, M. F. McCabe, and J. P. Evans (2011b), Developing an improved soil moisture dataset by blending passive and active microwave satellite-based retrievals, *Hydrol. Earth Syst. Sci.*, *15*, 425–436, doi:10.5194/hess-15-425-2011.

Liu, Y. Y., W. A. Dorigo, R. M. Parinussa, R. A. M. De Jeu, W. Wagner, M. F. McCabe, J. P. Evans, and A. I. J. M. Van Dijk (2012), Trend-preserving blending of passive and active microwave soil moisture retrievals, *Remote Sens. Environ.*, *123*, 280–297, doi:10.1016/j.rse.2012.03.014.

Njoku, E. G., T. J. Jackson, V. Lakshmi, T. K. Chan, and S. V. Nghiem (2003), Soil moisture retrieval from AMSR-E, *IEEE Trans. Geosci. Remote Sens.*, *41*(2), 215–229, doi:10.1109/TGRS.2002.808243.

Owe, M., R. de Jeu, and T. Holmes (2008), Multisensor historical climatology of satellite-derived global land surface moisture, *J. Geophys. Res.*, *113*, F01002, doi:10.1029/2007JF000769.

Parinussa, R., A. G. C. A. Meesters, Y. Y. Liu, W. Dorigo, W. Wagner, and R. A. M. De Jeu (2011), An analytical solution to estimate the error structure of a global soil moisture data set, *IEEE Geosci. Remote Sens.*, *8*(4), 779–783, doi:10.1109/LGRS.2011.2114872.

Rebel, K. T., R. A. M. de Jeu, P. Ciais, N. Viovy, S. L. Piao, G. Kiely, and A. J. Dolman (2012), A global analysis of soil moisture derived from satellite observations and a land surface model, *Hydrol. Earth Syst. Sci.*, *16*(3), 833–847, doi:10.5194/hess-16-833-2012.

Reichle, R. H., R. D. Koster, G. J. M. De Lannoy, B. A. Forman, Q. Liu, S. P. P. Mahanama, and A. Toure (2011), Assessment and enhancement of MERRA land surface hydrology estimates, *J. Clim.*, *24*(24), 6322–6338, doi:10.1175/JCLI-D-10-05033.1.

Robock, A., M. Mu, K. Vinnikov, I. V. Trofimova, and T. I. Adamenko (2005), Forty-five years of observed soil moisture in the Ukraine: No summer desiccation (yet), *Geophys. Res. Lett.*, *32*, L03401, doi:10.1029/2004GL021914.

Rodell, M., et al. (2004), The Global Land Data Assimilation System, *Bull. Am. Meteorol. Soc.*, *85*(3), 381–394, doi:10.1175/BAMS-85-3-381.

Sen, P. K. (1968), Estimates of the regression coefficient based on Kendall's tau, *J. Am. Stat. Assoc.*, *63*, 1379–1389, doi:10.1080/01621459.1968.10480934.

Sheffield, J., and E. F. Wood (2008), Global trends and variability in soil moisture and drought characteristics, 1950–2000, from observation-

driven simulations of the terrestrial hydrologic cycle, *J. Clim.*, *21*(3), 432–458, doi:10.1175/2007JCLI1822.1.

Simmons, A. J., K. M. Willett, P. D. Jones, P. W. Thorne, and D. P. Dee (2010), Low-frequency variations in surface atmospheric humidity, temperature, and precipitation: Inferences from reanalyses and monthly gridded observational data sets, *J. Geophys. Res.*, *115*, D01110, doi:10.1029/2009JD012442.

Taylor, C. M., R. A. M. De Jeu, F. Guichard, P. P. Harris, and W. A. Dorigo (2012), Afternoon rain more likely over drier soils, *Nature*, in press.

Tucker, C. J., J. E. Pinzon, M. E. Brown, D. A. Slayback, E. W. Pak, R. Mahoney, E. F. Vermote, and N. El Saleous (2005), An extended AVHRR 8-km NDVI dataset compatible with MODIS and SPOT vegetation NDVI data, *Int. J. Remote Sens.*, *26*(20), 4485–4498, doi:10.1080/01431160500168686.

Verdon-Kidd, D. C., and A. S. Kiem (2009), Nature and causes of protracted droughts in southeast Australia: Comparison between the Federation, WWII, and Big Dry droughts, *Geophys. Res. Lett.*, *36*, L22707, doi:10.1029/2009GL041067.

Zhu, C., and D. P. Lettenmaier (2007), Long-term climate and derived surface hydrology and energy flux data for Mexico: 1925–2004, *J. Clim.*, *20*(9), 1936–1946, doi:10.1175/JCLI4086.1.